ORIGINAL PAPER

AAV-mediated gene delivery of the calreticulin anti-angiogenic domain inhibits ocular neovascularization

Leilei Tu[1,2] · Jiang-Hui Wang[2,3] · Veluchamy A. Barathi[4,5,6] · Selwyn M. Prea[7] · Zheng He[7] · Jia Hui Lee[2] · James Bender[8] · Anna E. King[8] · Grant J. Logan[9] · Ian E. Alexander[9,10] · Youn-Shen Bee[11] · Ming-Hong Tai[12] · Gregory J. Dusting[2,3] · Bang V. Bui[7] · Jingxiang Zhong[1] · Guei-Sheung Liu[1,2,3,13,14]

Abstract

Ocular neovascularization is a common pathological feature in diabetic retinopathy and neovascular age-related macular degeneration that can lead to severe vision loss. We evaluated the therapeutic efficacy of a novel endogenous inhibitor of angiogenesis, the calreticulin anti-angiogenic domain (CAD180), and its functional 112-residue fragment, CAD-like peptide 112 (CAD112), delivered using a self-complementary adeno-associated virus serotype 2 (scAAV2) in rodent models of oxygen-induced retinopathy and laser-induced choroidal neovascularization. The expression of CAD180 and CAD112 was elevated in human umbilical vein endothelial cells transduced with scAAV2-CAD180 or scAAV2-CAD112, respectively, and both inhibited angiogenic activity in vitro. Intravitreal gene delivery of scAAV2-CAD180 or scAAV2-CAD112 significantly inhibited ischemia-induced retinal neovascularization in rat eyes (CAD180: 52.7% reduction; CAD112: 49.2% reduction) compared to scAAV2-mCherry, as measured in retinal flatmounts stained with isolectin B4. Moreover, the retinal structure and function were unaffected by scAAV2-CAD180 or scAAV2-CAD112, as measured by optical coherence tomography and electroretinography. Moreover, subretinal delivery of scAAV2-CAD180 or scAAV2-CAD112 significantly attenuated laser-induced choroidal neovascularization in mouse eyes compared to scAAV2-mCherry, as measured by fundus fluorescein angiography (CAD180: 62.4% reduction; CAD112: 57.5% reduction) and choroidal flatmounts (CAD180: 40.21% reduction; CAD112: 43.03% reduction). Gene delivery using scAAV2-CAD180 or scAAV2-CAD112 has significant potential as a therapeutic option for the management of ocular neovascularization.

Keywords Ocular neovascularization · Gene therapy · AAV · Calreticulin anti-angiogenic domain · Diabetic retinopathy · Neovascular age-related macular degeneration

Introduction

Ocular neovascularization is a common pathological feature in retinopathy of prematurity, proliferative diabetic retinopathy (PDR) and neovascular age-related macular degeneration (AMD); the latter two are leading causes of blindness in the industrialized world [1]. Retinal neovascularization (RNV) is caused by an initial phase of retinal microvessel loss and chronic hypoxia, which stimulates excess production of angiogenic factors that induce abnormal vessel growth. Aberrant vessel growth can ultimately lead to the formation of a fibrous scar and retinal detachment, which are associated with proliferative ischemic retinopathies, such as retinopathy of prematurity and PDR [2]. Choroidal neovascularization (CNV) that occurs in wet (exudative or neovascular) AMD originates from the choroid, whereby new vessels penetrate through Bruch's membrane into the retinal pigment epithelium and proliferate in the subretinal pigment epithelium and/or subretinal space. Newly formed vessels are susceptible to leakage, which can lead to rapid and severe vision loss when the macula is involved [3].

Vascular endothelial growth factor (VEGF) has been identified as a major contributor to RNV in ischemic

✉ Jingxiang Zhong
   zjx85221206@163.com

✉ Guei-Sheung Liu
   rickliu0817@gmail.com

Extended author information available on the last page of the article

retinopathies [4] and is known to be unregulated by hypoxia. VEGF both promotes the formation of new vessels and increases the permeability of existing vessels. Based on strong evidence, anti-VEGF agents are effective against RNV in patients with proliferative diabetic retinopathy [5]. The use of anti-VEGF agents has the potential to reduce the need for more destructive treatment modalities for PDR, such as panretinal laser photocoagulation. According to the results of a recent 2-year, randomized clinical trial, intravitreal injections of an anti-VEGF agent are at least as effective as panretinal laser photocoagulation in producing a sustained improvement in visual acuity [6].

VEGF also has an important role in CNV development in wet AMD, and intravitreal injections of anti-VEGF agents are now a first-line treatment for wet AMD [7]. However, the efficacy of anti-VEGF drugs can vary from person to person, and efficacy is currently difficult to predict before treatment [8]. Repeated injections, as often as monthly, are required to sustain efficacy due to the short half-life of current drugs [9]. The requirement for repeated intraocular injections carries a risk of sight-threatening complications, including inflammation, hemorrhaging, cataract formation, retinal detachment and potentially devastating intraocular infections (endophthalmitis) [10]. Thus, cheaper, safer, less-invasive and longer lasting alternative therapies are needed for the management of PDR and neovascular AMD.

The calreticulin anti-angiogenic domain (CAD180, formerly calreticulin-derived vasostatin), which comprises the N-terminal domain of calreticulin from amino acids 1–180 isolated from supernatants of an EBV-immortalized B cell line, is a potent inhibitor of angiogenesis [11, 12]. Based on our previous findings, the functional domain of CAD is a 48-amino acid fragment (residues 133–180), also known as CAD-like peptide 48 (CAD48). Topical application of CAD48 for 20 days attenuates vessel growth in rat eyes with laser-induced CNV [13, 14]. Recently, we constructed a CAD48 gene fused with the CAD signal peptide (residues 1–64) to enable extracellular secretion. This fusion gene (CAD112), when delivered via an adenoviral vector, also inhibits laser-induced CNV in rat eyes [15]. In this study, we evaluated the therapeutic efficacy of CAD180 and its functional 112-residue fragment, CAD112, delivered using a self-complementary adeno-associated virus serotype 2 (scAAV2) in rodent models of oxygen-induced retinopathy (OIR) and laser-induced CNV.

Results

## Delivery of the CAD180 and CAD112 genes inhibits angiogenic activities in vitro

The scAAV vectors encoding CAD180, CAD112 and mCherry were constructed (Fig. 1a) and packaged into an AAV2 capsid for gene delivery (Fig. 1b). Human umbilical vein endothelial cells (HUVECs) were transduced with scAAV2-mCherry, scAAV2-CAD180 or scAAV2-CAD112 at a multiplicity of infection (MOI) of 10^3 and 10^4 viral genomes/cell to validate the expression and anti-angiogenic activity of CAD180 and CAD112 delivered by scAAV2. Expression was examined by Western blotting using a calreticulin antibody, and anti-angiogenic function was evaluated using tube formation and cell migration assays (Fig. 2a). The 22-kDa CAD180 and 16 kDa CAD112 proteins were expressed in scAAV2-CAD180- and scAAV2-CAD112-transduced HUVECs, respectively (Figs. 2b and S1). Neither protein was detected in scAAV2-mCherry-transduced cells.

Compared with scAAV2-mCherry-transduced HUVECs, cells transduced with scAAV2-CAD180 or scAAV2-CAD112 showed less migration in the scratch migration assay (wound closure of cells transduced with scAAV2-mCherry: $64.8 \pm 4.6\%$ than cells expressing CAD180: $27.4 \pm 4.0\%$, $p < 0.01$; and CAD112: $32.3 \pm 3.1\%$, $p < 0.01$; $n = 14$; Fig. 2c). In addition, cells transduced with scAAV2-CAD180 or scAAV2-CAD112 formed significantly fewer tube-like networks, as evidenced by lower Matrigel lumen numbers (scAAV2-mCherry: 36.4 ± 7.9 compared with CAD180: 9.8 ± 2.4, $p < 0.01$; and CAD112: 12.8 ± 3.0, $p < 0.01$; $n = 9$) and branch points (scAAV2-mCherry: 134.3 ± 21.3 compared with CAD180: 65.0 ± 13.7, $p < 0.05$; and CAD112: 76.1 ± 11.9, $p < 0.05$; $n = 9$; Fig. 2d).

Efficacy of intravitreal scAAV2-mediated gene delivery in the rat retina

The effectiveness of scAAV2-mediated gene delivery was monitored in rats, and EGFP expression was evident across the whole flatmounted retina (Fig. 3a) and in all retinal layers in cryosections (Fig. 3b) 7 days after rats had received scAAV2-enhanced green fluorescent protein (EGFP) injection. P7 rat pups were intravitreally injected with scAAV2-mCherry, scAAV2-CAD180 or scAAV2-CAD112, and eyes were harvested at P18 to validate the expression of the mCherry, CAD180 and CAD112 genes (Fig. 3c). Retinal blood vessels were identified using isolectin B4 staining (green) and showed extensive overlap

Fig. 1 Schematic describing of scAAV2-mediated CAD180 and CAD112 gene delivery in the ocular neovascularization models. **a** Schematic diagram of the CAD180 and CAD112. CAD112 was generated by a fusing signal peptide (SP; 1-64 residues) with the anti-angiogenic domain (AD; 133–180 residues) of CAD180. *N* N-terminal domain. *C* C-terminal domain. *NF* non-functional domain. **b** Schematic diagram illustrating the production of scAAV2-CAD180, CAD112 or mCherry under control of the CMV promoter for intraocular gene delivery. mCH: mCherry
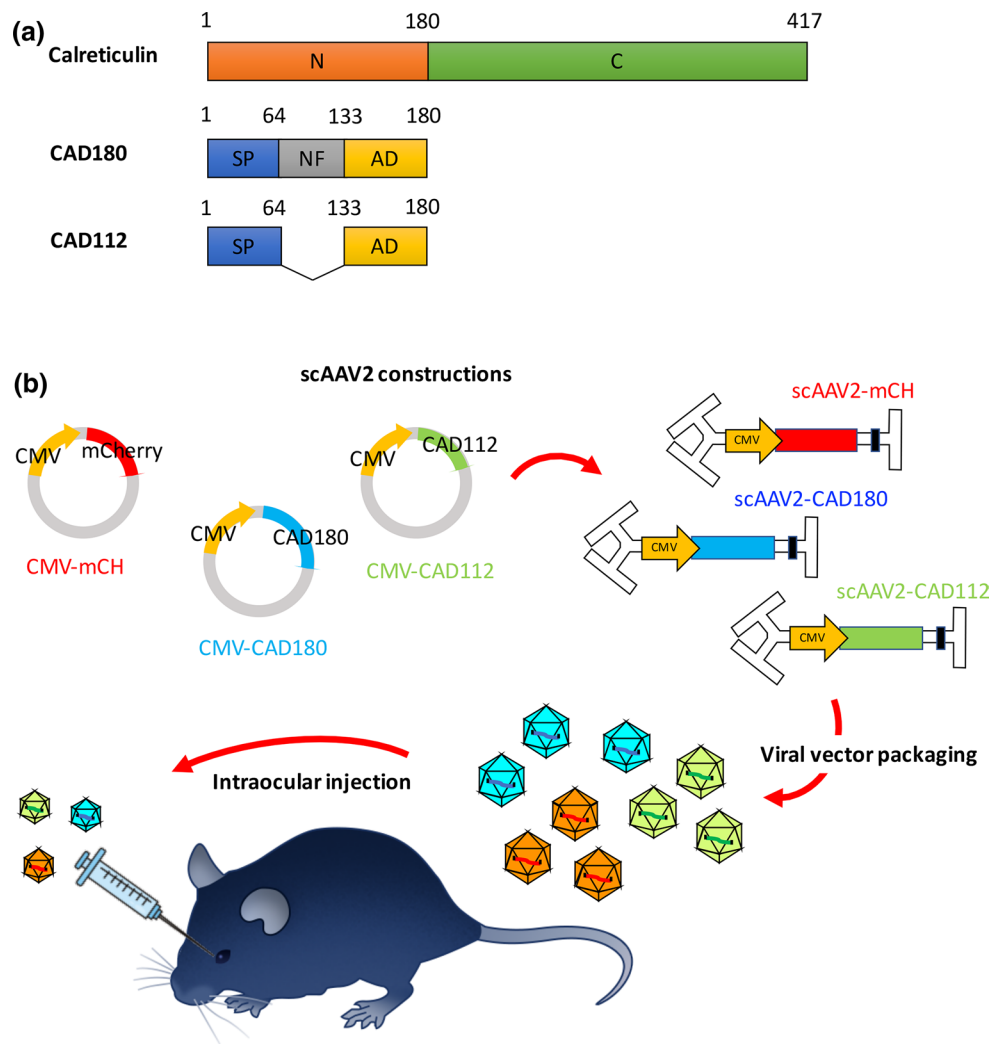
with transfected areas expressing mCherry (red) (Fig. 3d). Increased expression of the CAD180 or CAD112 mRNA in the retina of OIR rats was quantified using quantitative PCR. Compared with scAAV2-mCherry ($n = 3$), CAD180 expression was significantly increased (64,266-fold, $n = 4$) in retinas from scAAV2-CAD180-injected eyes. CAD112 expression was also significantly increased (93,348-fold, $n = 4$) in retinas from scAAV2-CAD112-injected eyes. A slight increase in CAD180 and CAD112 expression was observed in contralateral eyes (CAD180: 34.7-fold, $n = 4$; CAD112: 39.8-fold, $n = 4$; Fig. 3e).

Intravitreal delivery of the CAD180 and CAD112 genes attenuates RNV in an OIR rat model

The rat OIR model was employed to evaluate the therapeutic potential of scAAV2-CAD180 and scAAV2-CAD112 against retinal neovascularization. Small tufts of vascular endothelial cells were observed at the edge of new blood vessel growth adjacent to avascular areas. In some areas,

the tufts merged to form the neovascular brush boundary, which was characterized by darker staining. Tufts and brush borders were selected and marked in the enlarged images (Fig. 4a).

Compared with contralateral eyes (neovascular area: $2.40 \pm 0.18\%$, $n = 10$), intravitreal injection of scAAV2-CAD180 significantly inhibited neovascularization ($1.48 \pm 0.10\%$, $p = 0.004$; $n = 12$). Similarly, the scAAV2-CAD112 injection reduced the neovascular area ($1.42 \pm 0.11\%$, $p = 0.009$; $n = 10$) compared with contralateral eyes ($2.31 \pm 0.11\%$, $n = 10$). A significant difference was not observed between eyes injected with scAAV2-mCherry ($2.70 \pm 0.27\%$, $n = 11$) and the contralateral eyes ($2.24 \pm 0.16\%$, $p = 0.38$, $n = 12$) (Fig. 4b). Gene delivery via scAAV2-CAD180 or scAAV2-CAD112 significantly reduced the size of the OIR-induced neovascular area in rat eyes (CAD180: 52.7% reduction; CAD112: 49.2% reduction; $p < 0.001$, $n = 10–11$) compared with scAAV2-mCherry-injected eyes. A significant difference was not observed between eyes injected with scAAV2-CAD180 and

Fig. 2 Effects of scAAV2-mediated CAD180 and CAD112 gene delivery on angiogenic activity in vitro. **a** Schematic diagram of in vitro system to study the effectiveness of scAAV2-mediated CAD180 and CAD112 gene delivery. **b** Representative Western blot of the CAD180 or CAD112 protein expression in HUVECs transduced with scAAV2-mCherry, scAAV2-CAD180 or scAAV2-CAD112. Effects of the CAD180 and CAD112 gene delivery on cell migration (*c*; *n* = 14/group) and tube formation (*d*; *n* = 9/group) in HUVECs was quantified. Data are presented as mean ± SEM. Statistical analysis between groups was performed using one-way ANOVA followed by Tukey's multiple comparisons test (**$p < 0.001$, *$p < 0.05$). mCH: mCherry
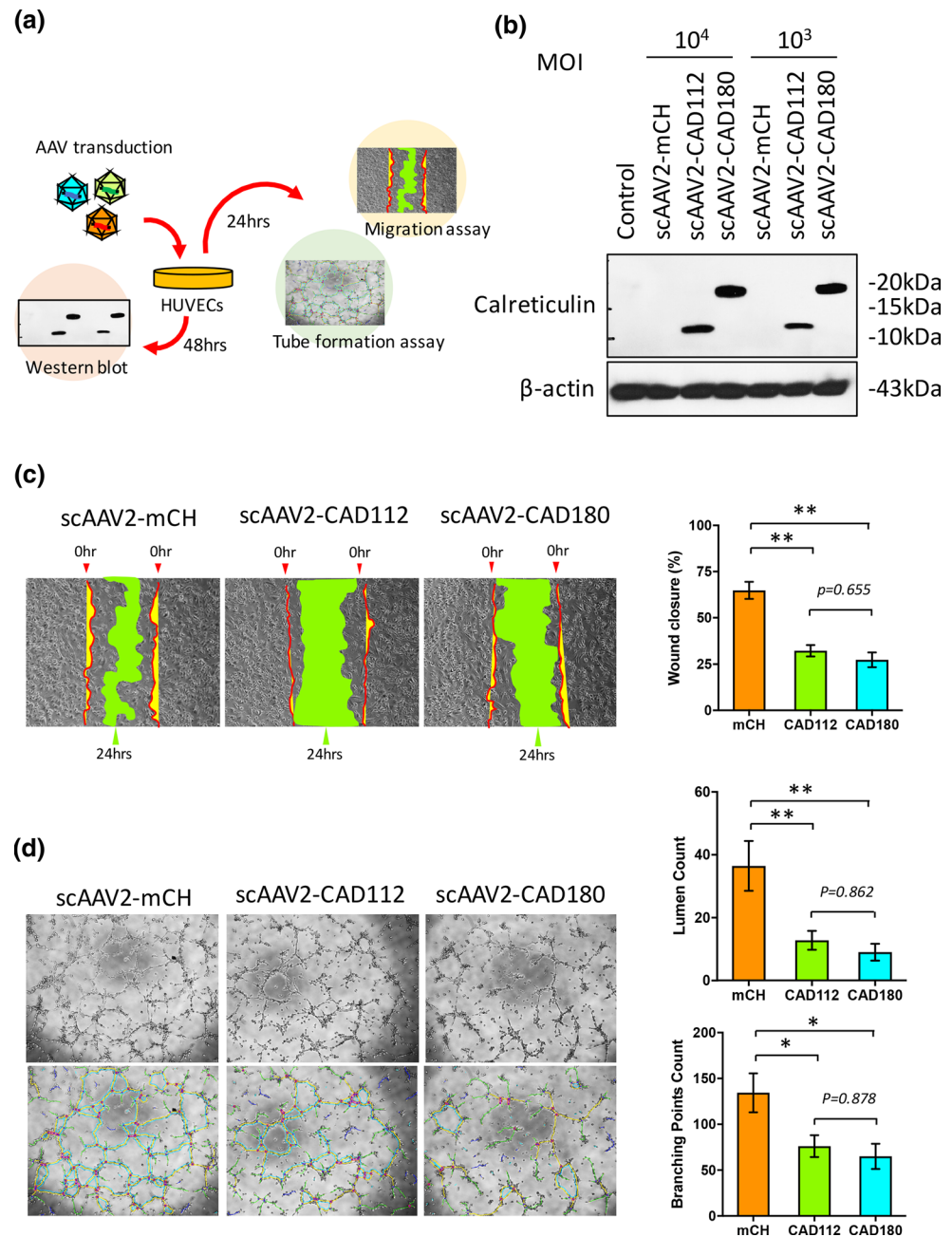
scAAV2-CAD112 ($p = 0.99$, $n = 10$–11) (Fig. 4b). A significant difference in avascular area was not observed between rats injected with scAAV2-mCherry (28.4 ± 4.4%) and those injected with scAAV2-CAD180 (24.5 ± 3.6%, $p = 0.67$) or scAAV2-CAD112 (38.6 ± 3.4%, $p = 0.47$) (Fig. 4c).

Effects of scAAV2-CAD180- and scAAV2-CAD112-mediated gene delivery on retinal structure and function in vivo

Electroretinography (ERG) and optical coherence tomography (OCT) were employed to evaluate the effects of intravitreal scAAV2-mediated delivery of the CAD180 or CAD112 gene on retinal function and structure in rats 28 days after the intravitreal injection (Fig. 5a). Group averaged waveforms elicited using bright and dim flashes of light from scAAV2-mCherry- (Fig. 5b), scAAV2-CAD112- (Fig. 5c) and scAAV2-CAD180-injected eyes (Fig. 5d) were very similar to the contralateral control eyes. Significant differences in the functions of photoreceptors ($p = 0.90$), bipolar cells ($p = 0.75$) or ganglion cells ($p = 0.10$) were not observed between scAAV2-CAD112-treated eyes and the contralateral controls (Fig. 5e–g). Likewise, the intravitreal
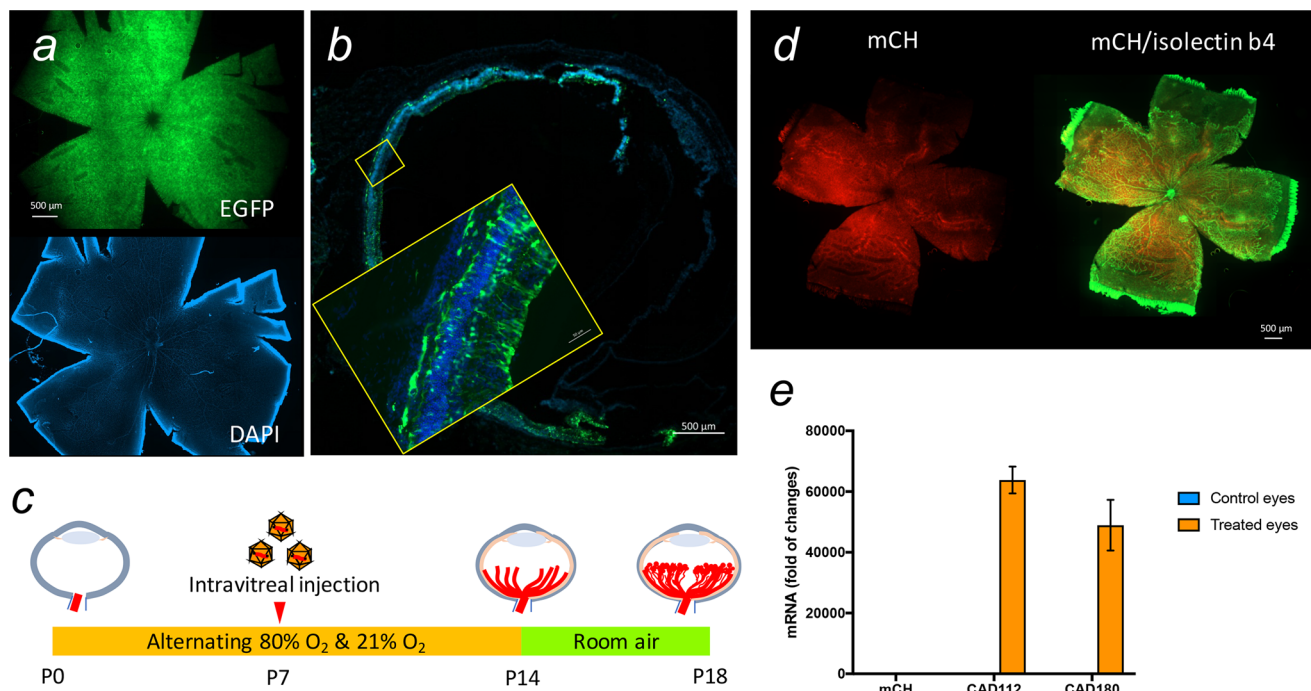
Fig. 3 Evaluation of the CAD180 and CAD112 expression after the intravitreal injections in rats. **a** 7 days after rats received the scAAV2-EGFP injection, EGFP expression was quantified in flatmounted retina also stained with DAPI. Scale bar: 500 μm. **b** Identification of EGFP expression in retinal cryosections also stained with DAPI. Scale bars: 500, 50 μm (middle-image). **c** Schematic diagram of rat OIR model protocol and timing of viral vector injection. Neonatal rats were exposed to daily cycles of 80% oxygen for 21 h and room air for 3 h from P0 to P14, after which animals were returned to room air until P18. ScAAV2-mCherry, scAAV2-CAD180 or scAAV2-CAD112 was injected at P7. **d** Identification of mCherry expression in the flatmounted retina from OIR rats at P18, also stained with isolectin B4. Scale bar: 500 μm. **e** qPCR quantification of CAD gene expression in the retinas of OIR rats at P18. Data are presented as mean ± SEM for 3–4 independent replicates. mCH: mCherry

injection of scAAV2-CAD180 did not significantly affect retinal function (photoreceptors, $p = 0.28$; bipolar cells, $p = 0.27$; ganglion cells, $p = 0.10$; Fig. 5e–g).

OCT was performed to evaluate the effects of scAAV2-mediated delivery of the CAD180 or CAD112 gene on retinal structure. The total retinal thickness was not different between vehicle- and scAAV2-injected eyes in all three groups (scAAV2-mCherry, $p = 0.10$; scAAV2-CAD180, $p = 0.16$; and scAAV2-CAD112, $p = 78$; Fig. 5h). Significant difference in the outer retinal (mCherry, $p = 0.38$; CAD180, $p = 0.95$; and CAD112, $p = 0.69$; Fig. 5i) and retinal nerve fiber layers (mCherry, $p = 0.07$; CAD180, $p = 0.18$; and CAD112, $p = 0.63$; Fig. 5j) was not observed between vehicle- and scAAV2-treated eyes in any of the groups. Thus, scAAV2-mediated delivery of the CAD180 or CAD112 gene via intravitreal injection does not lead to detectable adverse effects on retinal function and structure.

Subretinal delivery of CAD180 and CAD112 genes alleviates laser-induced CNV in mice

A mouse model of laser-induced CNV was employed to evaluate the therapeutic potential of scAAV2-CAD180 and scAAV2-CAD112 to prevent CNV. Seven days after the subretinal injection, laser surgery was performed to induce CNV in mice. The extent of choroidal vascularization was examined using fundus fluorescein angiography, and choroidal flatmounts were stained with isolectin B4 21 days after the subretinal injection (Fig. 6a). Images of CNV lesions were acquired at 3 and 5 min after the fluorescein injection (Fig. 6b). Quantification of the lesion area showed that compared with scAAV2-mCherry-injected eyes (9744 ± 2261 pixels, $n = 15$), mouse eyes that had received scAAV2-CAD180 showed significantly smaller CNV lesions (3251 ± 995 pixels, $p < 0.05$, $n = 13$; Fig. 6c). The scAAV2-CAD112-injected eyes also showed a similar reduction in the CNV lesion size (3668 ± 915 pixels, $p < 0.05$, $n = 20$; Fig. 6c). Reductions in the CNV lesion size were also confirmed in choroidal flatmounts stained with isolectin B4 (Fig. 6d). Compared with scAAV2-mCherry-injected eyes ($24,111 \pm 6146$ pixels, $n = 7$), mouse eyes that had received scAAV2-CAD180 or scAAV2-CAD112 had smaller CNV lesions (CAD180: $14,416 \pm 3151$ pixels, $n = 10$; CAD112: $13,736 \pm 6589$ pixels, $n = 4$; Fig. 6e).
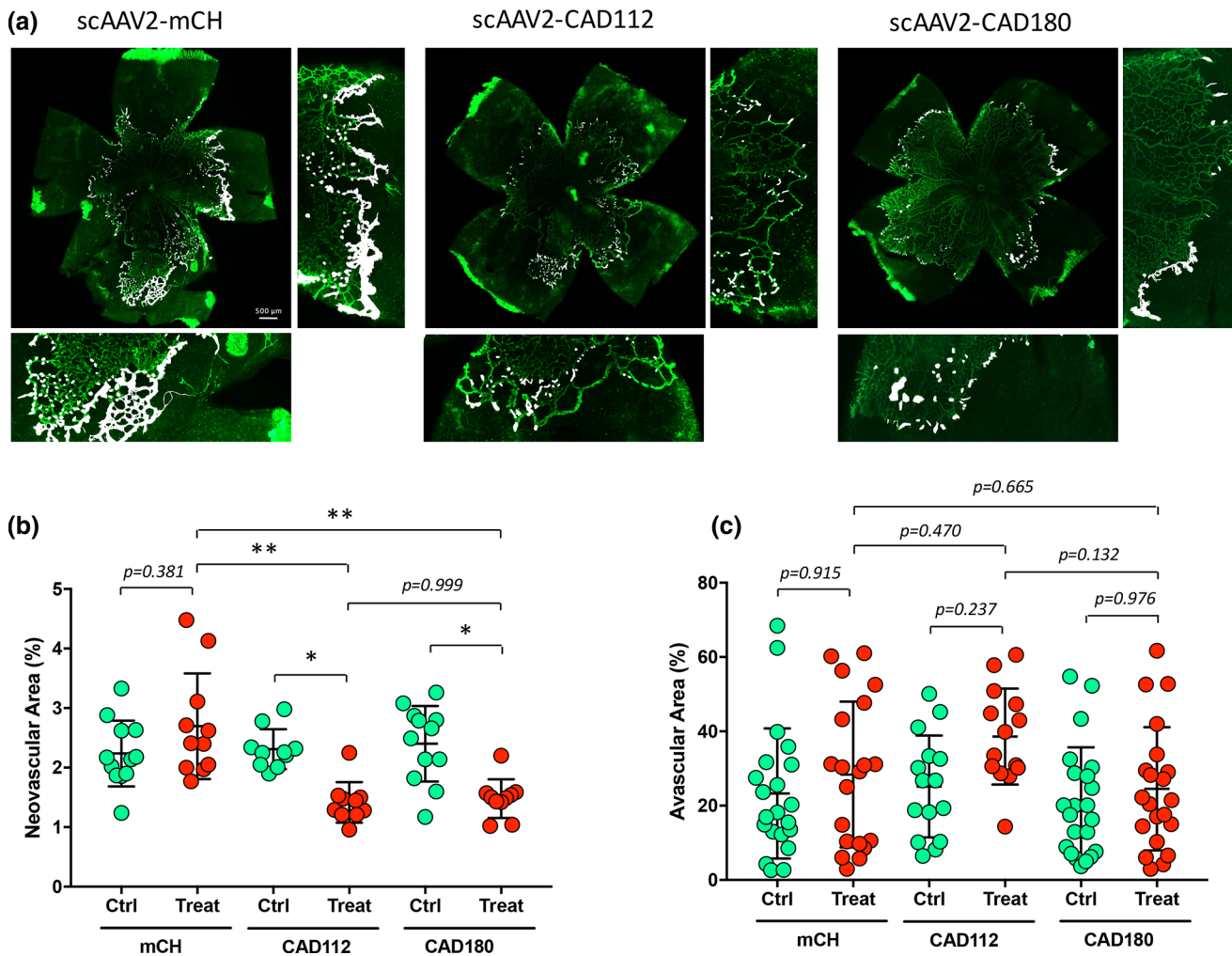
(a)

(b)

(c)

Fig. 4 Effects of intravitreal scAAV2-CAD180 and scAAV2-CAD112 injection on retinal neovascularization in the rat OIR model. **a** A typical cluster of vascular structures represented as "neovasculature" on a flatmounted retina at P18 after intravitreal injections at P7 stained with Isolectin B4. The retinal neovascular area was outlined for area quantification (white). Scale bar: 500 µm. **b** The retinal neovascular area was quantified for treated and control eyes from mCherry (control $n = 12$, treated $n = 11$), CAD180 (control $n = 10$, treated $n = 12$) and CAD112 (control $n = 10$, treated $n = 10$). Data are presented as mean $\pm$ SEM. **c** Retinal avascular area was quantified, and data are presented as mean $\pm$ SEM from 14 to 22 independent replicates. Statistical analysis between groups was performed using one-way ANOVA followed by Tukey's multiple comparisons test (**$p < 0.001$, *$p < 0.05$). mCH: mCherry

Discussion

Here, intraocular gene delivery of CAD180 or CAD112 via a robust self-complementary AAV2 vector reduced retinal and choroidal neovascularization. Specifically, CAD180 and CAD112 genes carried by a scAAV2 vector inhibited angiogenic activity in primary HUVECs in vitro. Furthermore, intravitreal delivery of the CAD180 or CAD112 gene attenuated OIR-induced RNV in rats. Finally, subretinal delivery of the CAD180 or CAD112 gene effectively attenuated the progression of laser-induced choroidal neovascularization in mice.

Gene therapy is an attractive therapeutic strategy and has shown promise for the treatment of eye disease and the prevention of blindness [16]. One advantage is that it is easier and less costly to manufacture gene therapy vectors than to produce large amounts of purified proteins. Based on data from recent clinical trials, gene therapy using anti-VEGF agent such as sFlt-1, a soluble form of the Flt-1 receptor, can benefit patients with neovascular AMD [17, 18]. A key advantage of our CAD-based gene therapy compared to current therapeutic approaches (e.g., anti-VEGF antibody injections or sFlt-1 gene therapy) for ocular neovascularization is that it specifically targets endothelial cells and is thus less likely to exhibit toxicity toward other cells [19–21]. Moreover, CAD also has anti-inflammatory properties, which will help control inflammation [22], a major contributor to the ongoing drive

Fig. 5 Effects of intravitreal scAAV2-CAD180 and scAAV2-CAD112 injection on retinal function and structure. **a** ERG and OCT were assessed 28 days following intravitreal drug injection. **b** Average dim and bright flash ERG traces from the vehicle (black traces, $n = 8$) and scAAV2-mCherry-injected (red traces, $n = 8$) eyes. **c** Average ERG traces from the vehicle (black traces, $n = 8$) and CAD112 (blue traces, $n = 8$) injected eyes. **d** Average ERG traces from the vehicle (black traces, $n = 7$) and CAD180 (green traces, $n = 7$) injected eyes. **e** Group average ($\pm$ SEM) photoreceptoral response amplitude from mCherry (red, $n = 8$) and CAD112 (blue, $n = 8$) and CAD180 injected eyes (green, $n = 7$) as well as their fellow vehicle-injected eyes. **f** Group average bipolar cell response amplitude. **g** Group average ganglion cell response amplitude. **h** Group average total retinal thickness. **i** Group average outer retinal thickness. **j** Group average retinal nerve fiber layer thickness. Data are presented as mean $\pm$ SEM. Statistical analysis between injected and control eyes was performed using two-tailed Student t test. mCH: mCherry
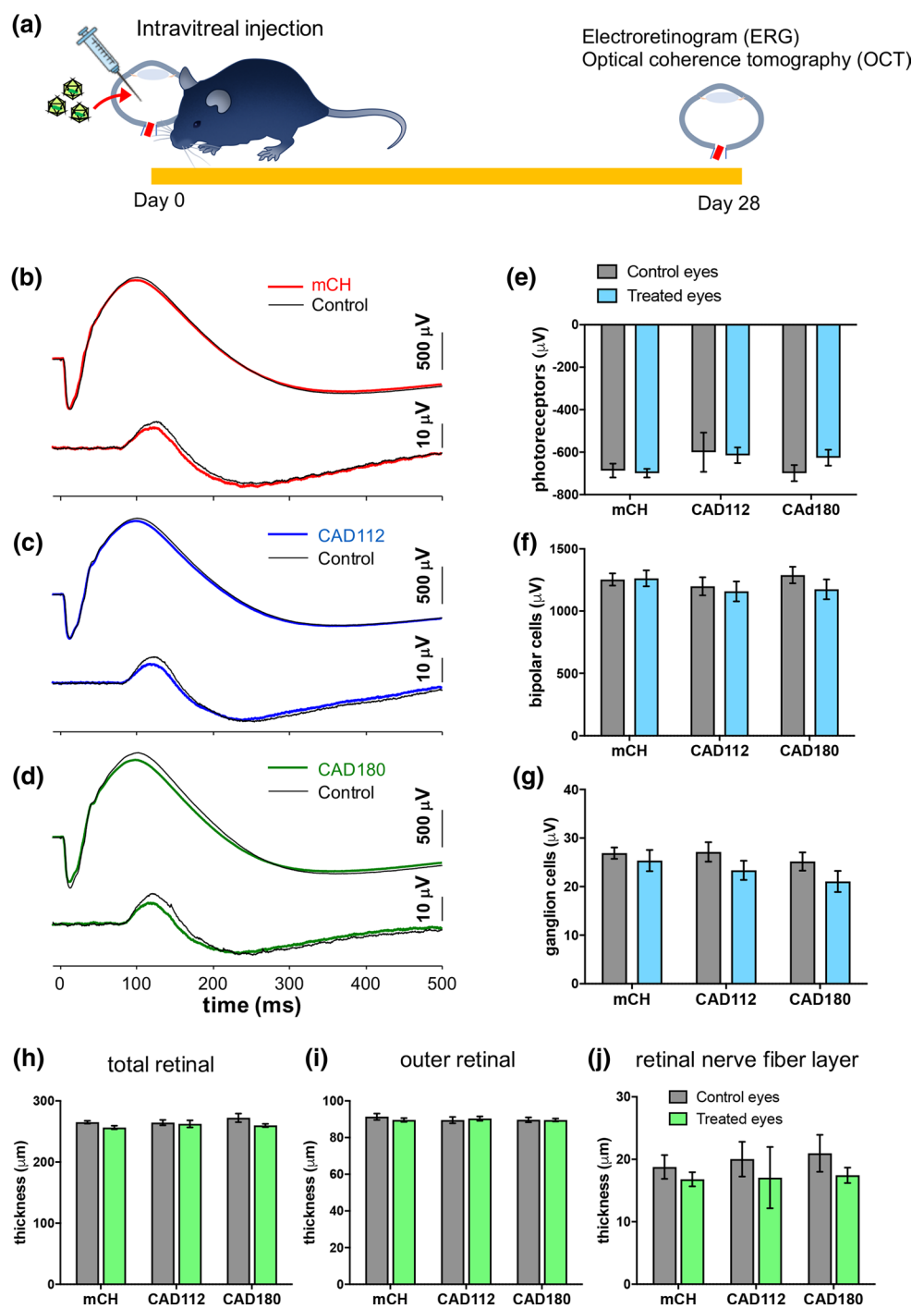
for neovascularization in both patients with DR [23] and AMD [24]. In addition, the CAD180 and CAD112 treatments provided similar benefits in reducing neovascular NV tufts and choroidal neovascular lesions, suggesting that the difference in molecular weight did not modify their anti-angiogenic properties. Low molecular weight therapeutic proteins such as CAD112 might have additional benefits in terms of better tissue diffusion and penetration and thus bioavailability.

The effectiveness of anti-angiogenic drugs is highly dependent on the drug delivery method and its capacity to produce sustained expression of the therapeutic molecule. As shown in our previous study, delivery of the CAD112 gene via an adenoviral vector significantly attenuates the development of laser-induced CNV in rat eyes [15]. Although subconjunctival injection of adenoviruses is safe and induces only a mild, transient local immune response [25], gene expression was not maintained for more than

Fig. 6 Effect of subretinal scAAV2-CAD180 or scAAV2-CAD112 injection on laser-induced CNV in mice. **a** A schematic diagram of the time-line for the laser-induced CNV mouse model and injection of viral vectors. Choroidal vascularity of laser-induced CNV lesions was examined by FFA and choroidal flatmount staining with isolectin B4 at 21 days after subretinal injection. **b** Representative CNV lesions in mouse eyes treated with scAAV2-mCherry ($n = 17$), scAAV2-CAD180 ($n = 13$) or scAAV2-CAD112 ($n = 20$) were identified by FFA. **c** Average ($\pm$ SEM) CNV lesions from fluorescein angiography for the three groups. **d** Representative profile of isolectin B4-stained blood vessels in the choroidal flatmounts. The CNV area was quantified (outline). Scale bar: 200 μm. **e** Average ($\pm$ SEM) CNV area from flatmounts for the three groups ($n = 4–10$). Statistical analysis between groups was performed using one-way ANOVA followed by Tukey's multiple comparisons test (*$p < 0.05$). mCH: mCherry
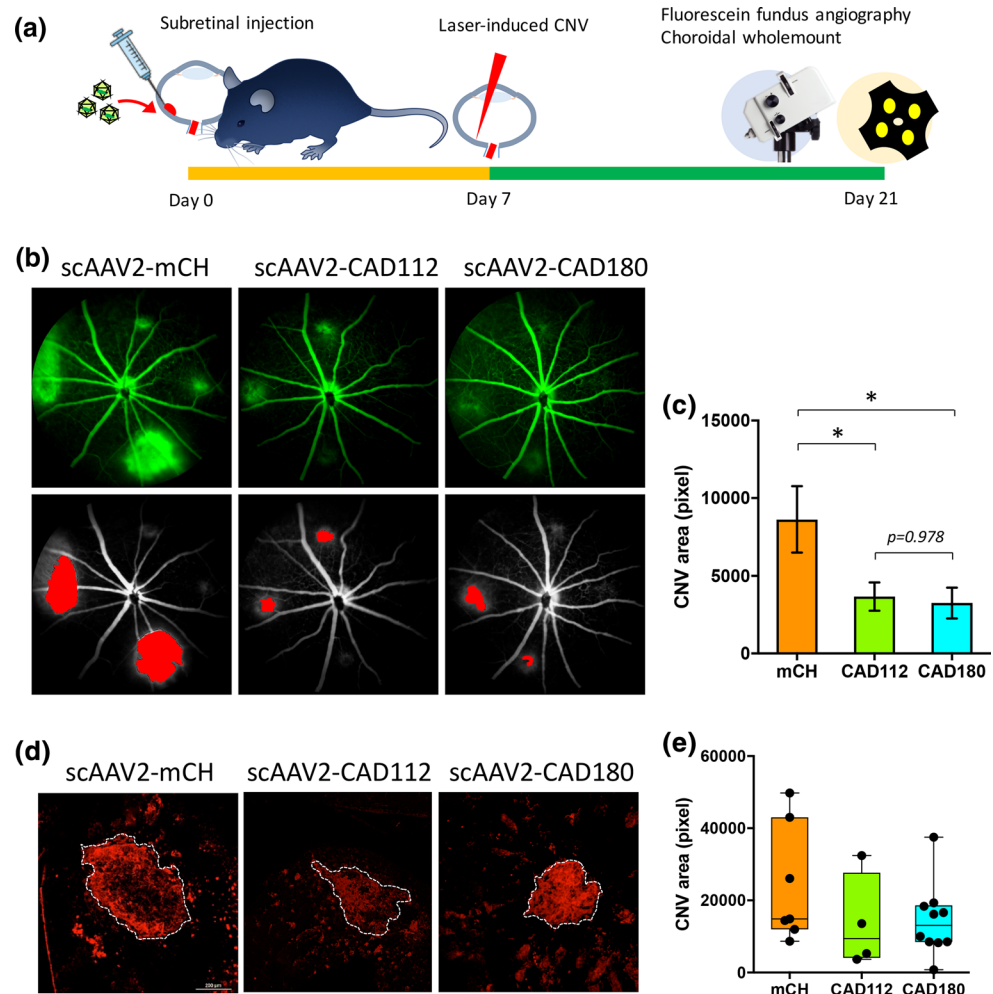
112 days using this delivery route. Moreover, subconjunctival injections produce lower transgene expression in the retina and choroid than intravitreal injections. We employed a self-complementary AAV vector in the present study to produce persistently high levels of transgene expression for long periods. The scAAV vector has been shown to exhibit improved transduction efficiency in the retina compared to conventional single-stranded AAV vectors [26]; it is also faster, requiring only 48 h to initiate gene expression [27]. Indeed, our data indicate rapid onset of gene expression in rats, as evidenced by the widespread expression of EGFP 7 days after a single intravitreal injection of scAAV2-EGFP. Rapid-onset gene expression was also confirmed by widespread expression of mCherry in retinal flatmounts and increased retinal expression of the CAD180 or CAD112 mRNA 11 days after injection. Thus, scAAV2-mediated delivery of the CAD180 and CAD112 gene effectively targets pathological vessels in a range of disease models.

Intravitreal and subretinal injection routes were used to evaluate the therapeutic potential of scAAV2-mediated CAD180 and CAD112 gene delivery for treatment of retinal and choroidal neovascularization, respectively. Intravitreal injections are routinely used to administer pharmacological treatments to the eye and theoretically allow the vector to be exposed to a wide retinal area via the vitreoretinal surface, which is beneficial in targeting RNV. However, based on observations in animal models, intravitreal delivery using single-stranded AAV2 does not provide a high transduction efficiency in the outer retinal layers, suggesting that a barrier to vector diffusion may exist [28, 29]. Therefore, subretinal gene delivery may target choroidal neovascularization with better efficacy. Subretinal injections are widely used in clinical retinal gene therapy trials [18, 30, 31] and appear to induce a lower immune reaction than intravitreal delivery [32]. However, the surgery used to access the subretinal space is associated with a greater risk. The development of native and engineered AAV capsids with greater tropism for desired target cells types and better retinal penetration will further accelerate the potential for human retinal gene therapy. For example, intravitreal delivery via AAV-7m8 [33], which contains a capsid that has been modified to enhance retinal

penetration, might be a more viable option for targeting the outer retinal layers and choroid.

Adverse effects associated with prolonged expression of vascular targeting proteins by viral vectors must be excluded. Although anti-VEGF therapies have revolutionized the treatment of neovascular AMD and DR [17, 18, 34, 35], the systemic safety of repeated anti-VEGF injections is raising increasing concerns. In particular, cerebrovascular accidents and death have been noted in young patients with diabetic macular edema who were treated with intravitreal injections of anti-VEGF agents [36, 37]. Using in vivo ERG assessment and OCT imaging, we showed that intravitreal scAAV2-CAD180 or scAAV2-CAD112 injections had little effect on retinal function and structure over the course of 28 days. The long-term safety of CAD180 and CAD112 gene delivery will need to be confirmed before their translation into clinical trials.

In summary, scAAV2-mediated CAD180 or CAD112 gene therapy reduces ocular neovascularization. Although further investigations are required to assess long-term safety and efficacy, our data suggest that scAAV2-mediated delivery of the CAD180 or CAD112 gene may be a viable therapeutic alternative for retinal and choroidal neovascularization, as it requires a single injection and can thus avoid the risks associated with the frequent injections required for current therapies.

Materials and methods

Cell culture

HUVECs were purchased from Lonza (catalog no. CC-2519; Lonza, Walkersville, MD, USA) and cultured in endothelial cell basal medium-2 (EBM-2) supplemented with the EGM™-2 BulletKit™ (catalog no. CC-5035; Lonza). HEK293A cells were purchased from Invitrogen (catalog no. R70507; Life Technologies Australia, Mulgrave, VIC, Australia) and cultured in Dulbecco's Modified Eagle's Medium (DMEM) (catalog no. 11965118; Life Technologies Australia) supplemented with 10% fetal calf serum (Sigma-Aldrich, St. Louis, MO, USA), 2 mM glutamine (catalog no. 2503008; Life Technologies Australia), and 50 U/mL penicillin–streptomycin (catalog no. 15070063; Life Technologies Australia). Both cell lines were cultured in a humidified 5% CO_2 atmosphere at 37 °C.

AAV viral vector

The scAAV2 vectors encoding mCherry (scAAV2-mCherry), CAD180 (scAAV2-CAD180), and CAD112 (scAAV2-CAD112) used in this study were packaged as previously described [34]. Briefly, the mCherry, CAD180 and CAD112 cDNAs surrounded by AgeI and NotI cleavage sites were obtained by PCR and subcloned into the pHpa-trs-SK plasmid under control of the cytomegalovirus (CMV) immediate early promoter (kindly provided by Douglas M. McCarty, Center for Gene Therapy, Nationwide Children's Hospital, USA) [38]. The scAAV2 vectors were prepared by transfecting HEK293 cells with the pHpa-trs-SK/mCherry, pHpa-trs-SK/CAD180 or pHpa-trs-SK/CAD112 plasmid, helper plasmid (pXX6) and AAV2 capsid plasmid (pXX2) using the calcium phosphate method. Viral vectors were purified with the AAV2pro Purification Kit (catalog no. 6232; Clontech Laboratories, Mountain View, CA, USA) 48 h after viral transduction. Vector genome titers were determined by real-time quantitative PCR.

Western blot analysis

Forty-eight hours after cells were transduced with scAAV2-mCherry, scAAV2-CAD180 or scAAV2-CAD112 at an MOI of 10^3 and 10^4; HUVECs were washed with cold phosphate-buffered saline (PBS) and collected in the lysis buffer (50 mM Tris–HCl, pH 7.4, 1% NP-40, 0.25% sodium deoxycholate, 150 mM NaCl, and Complete Protease Inhibitor Cocktail [catalog no. 11697498001; Sigma-Aldrich]). Proteins were separated using NuPAGE™ Novex™ 4–12% Bis–Tris Protein Gels (catalog no. NP0321BOX; Life Technologies Australia) and transferred to polyvinylidene fluoride membranes (catalog no. IPVH00010; Immobilon-P; Millipore, Billerica, MA, USA) using the XCell II™ Blot Module (Life Technologies Australia). Membranes were blocked with 5% skim milk in TBS-T (10 mM Tris, 150 mM NaCl, and 0.05% Tween-20) at room temperature for 1 h and then incubated with a mouse monoclonal calreticulin (FMC75) antibody (1:1000 dilution; catalog no. ADI-SPA-601-D; Enzo Life Sciences, Farmingdale, NY, USA) overnight at 4 °C or mouse monoclonal actin (clone C4) antibody (1:2000 dilution; catalog no. MAB1501; Millipore) at room temperature for 1 h. Membranes were washed, further incubated with a horseradish peroxidase-conjugated goat anti-mouse secondary antibody (1:5000 dilution; catalog no. A-11045; Life Technologies Australia) at room temperature for 1 h, and developed using the Amersham ECL Prime Western Blotting Detection Kit (catalog no. RPN2232; GE Healthcare Australia, Parramatta, NSW, Australia).

Cell migration assay

HUVECs were seeded onto 6-well plates at a density of 2.5×10^5 cells/well and transduced with scAAV2-mCherry, scAAV2-CAD180 or scAAV2-CAD112 at a MOI of 1000 vg/cell for 48 h. Confluence was greater than 80% prior to the scratch assay. A 200-μL pipette tip was used to press firmly against the top of the tissue culture

plate and make a vertical wound by passing the tip down through the cell monolayer to create three straight lines with two crosses lacking cells in each well, and the debris was removed by replacing the media with 2 mL of EBM-2 supplemented with EGM™-2 BulletKit™. Four images of each well were captured immediately after scraping and after a 24-h incubation period. Areas without cells were measured using ImageJ version 1.48 software (http://imagej.nih.gov/ij/; provided in the public domain by the National Institutes of Health, Bethesda, MD, USA).

Tube formation assay

Tube formation was quantified using a previously described method [39]. Briefly, BD Matrigel™ Basement Membrane Matrix (catalog no. 356234; Becton–Dickinson; Bedford, MA, USA) was warmed to room temperature and transferred to ice; the liquid was incubated on ice for at least 10 min until it was completely thawed. Then, 50 µL of Matrigel were added to each well of a horizontal 96-well plate to allow the Matrigel to distribute evenly, and incubated at 37 °C for 30 min. HUVECs were transduced with scAAV2-mCherry, scAAV2-CAD180 or scAAV2-CAD112 at an MOI of 1000 vg/cell for 48 h. Cells (1.5×10^4) were re-suspended in EBM-2 and loaded on the top of the Matrigel. Following a 6-h incubation at 37 °C, each well was photographed under a microscope. The numbers of endothelial tube lumens were counted in three replicate wells using Angiogenesis Analyzer in ImageJ version 1.48 software [40].

Animals

Ethical approval for the experiments performed in this study was obtained from the Animal Ethics Committee of the University of Melbourne, St. Vincent's Hospital, and Singapore Eye Research Institute. All experimental procedures performed on rats and mice adhered to the Association for Research in Vision and Ophthalmology Statement for the Use of Animals in Ophthalmic and Vision Research.

All animals were supplied by the Animal Resources Centre (Perth, Western Australia, Australia) and were housed at the Experimental Medical and Surgical Unit, St. Vincent's Hospital (East Melbourne, Victoria, Australia) and Melbourne Brain Centre (Parkville, Victoria, Australia). Animals were housed in standard cages, with free access to food and water in a temperature-controlled environment under a 12-h light (50 lux illumination) and 12-h dark (< 10 lux illumination) cycle to minimize possible light-induced damage to the eye.

Rat model of oxygen-induced retinopathy

The OIR model was established as previously described [41]. Briefly, Sprague–Dawley prepartum female rats were ordered and received at approximately 13 or 14 days of gestation. After parturition, the mother and the newborn pups were placed in the oxygen chamber, and a specific oxygen exposure protocol (daily exposure to 80% oxygen for 21 h and a return to room air for 3 h) was initiated. Mothers and newborn pups remained in the oxygen chamber for 14 days. The normal lighting cycle and standard room temperature were maintained. At 14 days postpartum, mothers and pups were removed from the oxygen chamber and placed in an air-conditioned room for 4 days. At 18 days postpartum, mothers and pups were euthanized with CO_2, and eyes (only pups) were harvested for histological and biochemical evaluations.

Intravitreal injection

The scAAV2 vectors were intravitreally injected at postnatal day 7 (P7) within the 3 h window during which animals remained in ambient air. Rats were anesthetized with isoflurane (1.5–2 mL/min). Intravitreal injections were performed under a surgical microscope. After a small puncture through the conjunctiva and sclera was created using a 30 gauge needle, a hand-pulled glass micropipette connected to a 10-µL Hamilton syringe (Bio-Strategy, Broadmeadows, VIC, Australia) was inserted into the vitreous and 1 µL of scAAV2-mCherry (7.5×10^8 vg/µL), scAAV2-CAD180 (8.0×10^8 vg/µL) or scAAV2-CAD112 (6.1×10^8 vg/µL) was injected into one eye of each rat using a UMP3-2 Ultra Micro Pump (World Precision Instruments, Sarasota, FL, USA) at a rate of 100 nL/s. Animals were monitored until full recovery and then returned to the oxygen chamber. Any issues with the injection, including large backflow upon removal of the needle and hemorrhaging of external or internal vessels, were noted, and those eyes were excluded from the analysis.

Quantitative PCR

Total RNA was extracted from retinas and purified using commercial kits according to the manufacturer's instructions (catalog no. 74104; RNeasy Mini Kit; Qiagen, Chadstone, VIC, Australia). Briefly, each retina was homogenized, and total RNA was purified with a column system. Total RNA (100 ng) was then reverse-transcribed to cDNAs using a high-capacity RT kit (catalog no. 4374996; Life Technologies Australia). Quantitative PCR was performed using Fast SYBR Green Master Mix (catalog no. 4385612; Life Technologies Australia) with CAD primers (F: 5′-GGATCGAATCCAAACACAAGTC; R: 5′-ATCAGTGTGTACAGGTGTGTAA) for CAD180 and CAD112. Rat GAPDH was

used as a reference gene and amplified with GADPH primers (F: 5′-GAGTCAACGGATTTGGTCGT; R: 5′-TTGATT TTGGAGGGATCTCG). For the analysis of mRNA expression, relative expression levels of CAD180 or CAD112 in retinas from different rats administered scAAV2-mCherry, scAAV2-CAD180 or scAAV2-CAD112 and their contralateral control eyes were calculated using the $^{\Delta\Delta}$Ct method, as previously described by Livak [42].

Retinal flatmounting and isolectin B4 staining

Eyes were fixed with 4% PFA for 60 min and dissected under a dissection microscope. Retina–choroid–sclera flatmounts with four equally spaced radial relaxing incisions extending two-thirds of the way from the retinal periphery to the optic nerve head were obtained by hemisecting the eye, and the cornea, iris and lens were discarded. The sclera and choroid were removed, leaving only the retina, and the residual vitreous and hyaloid vessels were teased away using fine forceps.

The fully dissected retina was first permeabilized with PBS-Triton X-100 for 30 min and then washed twice with PBS. Alexa Fluor™ 488-conjugated isolectin B4 (isolectin GS-IB4 from *Griffonia simplicifolia*; catalog no. I21411; Life Technologies Australia) that specifically binds to α-glycosylated glycoprotein residues on vascular endothelial cells and macrophages was diluted in PBS (4 µg/mL) and added to each retina in the dark at 4 °C overnight. The stained retina was washed five times with PBS on the next morning and carefully flatmounted on a slide using fluorescence mounting medium (catalog no. s3020; DAKO, Carpinteria, CA, USA).

Quantification of RNV by imaging retinal flatmounts

Images were digitized using a fluorescence microscope (Zeiss Axio Imager Microscope; Carl-Zeiss-Strasse, Oberkochen, Germany) equipped with a charge-coupled digital camera (Axiocam MRm, Zeiss) and image acquisition software (ZEN2, Zeiss). The entire retina was photographed using an appropriate filter for the fluorescence emission spectra of mCherry (610 nm) and isolectin B4 (509 nm), and separate images were merged to form a complete image of the retina.

Early stages of RNV were observed as small tufts of vascular endothelial cells, which always occurred near the edge of the developing vasculature, immediately adjacent to the avascular area. In some areas, the initial tufts merged to form the RNV brush boundary, which is characterized by dark staining. Images were analyzed using Photoshop to select and mark tufts and the brush borders in enlarged images, and the area of the retina with RNV was calculated and expressed as a percentage of the total retinal area. Simultaneously, the avascular area was quantified and expressed

as a percentage of total retinal area [43]. The quantitative analysis was performed by two assessors who were blinded to the groups.

Electroretinography (ERG)

Twenty-eight days after the injection, rats underwent and overnight dark adaptation (~ 12 h), followed by an electroretinography assessment in the dark. Details of the functional assessment have been previously reported [44], with the exception that the reference chloride silver electrode was placed around the outside of the eye. As previously described [44], the ERG analysis returned the photoreceptor- (a-wave), bipolar cell- (b-wave), and ganglion cell-dominant (scotopic threshold response, STR) components of the ERG waveform. Group data are provided as the means (± standard errors of the means).

Spectral-domain optical coherence tomography (SD-OCT)

Following the ERG measurement, rat eyes were imaged using SD-OCT (Bioptigen, Inc., Morrisville, NC, USA). Volume scans consisting of 1000 A-scans per 100 B-scans (equally spaced across the 1.4 mm vertical dimension) centered on the optic nerve head (ONH; $1.4 \times 1.4 \times 1.57$ mm) were obtained from both eyes. OCT images were analyzed using FIJI software (provided in the public domain by the National Institutes of Health, Bethesda, MD, USA). OCT images including the optic nerve were manually segmented by a grader who was blinded to the groups, as previously described [42]. The total retinal thickness (TRT) was measured from the inner limiting membrane to Bruch's membrane. The thickness of the retinal nerve fiber layer (RNFL) was measured from the inner limiting membrane to the inner aspect of the inner plexiform layer. Outer retinal thickness was measured from Bruch's membrane to the outer plexiform layer.

Mouse model of laser-induced choroidal neovascularization

C57BL/6 J mice were anesthetized with a combination of ketamine (20 mg/kg body weight) and xylazine (2 mg/kg body weight). After pupil dilation via the topical administration of 1% tropicamide (Alcon Laboratories, Fort Worth, TX, USA) and 2.5% phenylephrine (Bausch and Lomb Pharmaceuticals, Inc., Tampa, FL, USA) ophthalmic solutions to the surface of the eye, laser photocoagulation was performed using the image-guided laser system (Micron IV, Phoenix Research Laboratories, Pleasanton, CA, USA). Four laser burns were generated in each eye at the 3, 6, 9 and 12 o'clock

positions located at equal distances from the optic disk using a green Argon laser pulse with a wavelength of 532 nm, a fixed diameter of 50 μm, a duration of 50 ms and a power of 120 mW. Mice were kept warm under an infrared light after the laser treatment until they recovered from anesthesia.

Subretinal injections

C57BL/6 J mice were anesthetized with a combination of ketamine (20 mg/kg body weight) and xylazine (2 mg/kg body weight). Pupils were dilated via the topical application of mydriatic agents: 1% tropicamide (Alcon Laboratories) and 2.5% phenylephrine (Bausch and Lomb Pharmaceuticals). The posterior eye was observed under a stereoscopic surgical microscope by applying a drop of Vidisic ophthalmic gel (Dr Mann Pharma, Germany) and placing a round cover glass of 12 mm in diameter over the cornea to perform subretinal injections. A small incision was carefully made 1 mm behind the limbus using a sharp 30 gauge needle. A blunt 36 gauge needle (World Precision Instrument) attached to a microliter glass syringe was then gently inserted through the incision into the subretinal space. Then, 1 μL of the AAV suspension containing scAAV2-mCherry (7.5×10^9 vg/μL), scAAV2-CAD180 (8.0×10^8 vg/μL), or scAAV2-CAD112 (6.1×10^8 vg/μL) was administered into the subretinal space. Successful subretinal delivery was confirmed by the presence of a bleb at the injection site. Any issues related to the injection were noted, and if necessary, eyes were excluded from the analysis.

Fundus fluorescein angiography (FFA)

Color fundus photography and FFA were performed with a rodent retinal imaging system (Micron IV, Phoenix Research Labs) on days 7 and 14 after laser photocoagulation. Mice were anesthetized with a combination of ketamine (20 mg/kg body weight) and xylazine (2 mg/kg body weight), and then pupils were dilated via the topical administration of 1% tropicamide (Alcon Laboratories) and 2.5% phenylephrine (Bausch and Lomb Pharmaceuticals) ophthalmic solutions. Fundus photographs were acquired, after which 10% sodium fluorescein dye was intraperitoneally injected at a dose of 0.01 mL/5 g body weight. Fluorescent images were immediately acquired through a blue filter and at 3 and 5 min after the fluorescein injection. The area of leakage and the intensity of the CNV lesions were graded using ImageJ version 1.48 software by observers who were blinded to the groups.

Quantification of CNV lesions using choroidal flatmount imaging

Mice were euthanized 21 days after laser photocoagulation. Eyes were immediately enucleated and fixed with 4% paraformaldehyde in 1X PBS for 1 h at room temperature. Eyes were dissected carefully, and the retina and choroid/retinal pigment epithelium were mounted separately on microscopic slides. Flatmounts were placed in chilled 70% ethanol for 20 min, rinsed with PBS and permeabilized with 1% Triton X/PBS for 30 min at room temperature. Flatmounts were then incubated with a 1:1000 dilution of Alexa Fluor 594-conjugated isolectin GS-IB4 (*Griffonia simplicifolia*) (catalog no. I21413; Molecular Probes, Eugene, OR, USA) overnight at 4 °C. Stained tissues were mounted with Prolong Gold (catalog no. P36930; Life Technologies Australia) and incubated overnight in the dark. Flatmounts were imaged with a laser-scanning confocal fluorescence microscope. The CNV lesion area was measured by observers who were blinded to the groups using ImageJ version 1.48 software.

Statistical analysis

Data are expressed as the means $\pm$ standard errors of the means (SEM). Means were analyzed with an unpaired, two-tailed Student's *t* test or one-way analysis of variance (ANOVA), followed by Tukey's post hoc test (GraphPad Prism software version 7.0). A value of $p < 0.05$ was considered statistically significant.

Compliance with ethical standards

References

1. Campochiaro PA (2000) Retinal and choroidal neovascularization. J Cell Physiol 184(3):301–310. https://doi.org/10.1002/1097-4652(200009)184:3<301:AID-JCP3>3.0.CO;2-H

2. Sapieha P, Hamel D, Shao Z, Rivera JC, Zaniolo K, Joyal JS, Chemtob S (2010) Proliferative retinopathies: angiogenesis that blinds. Int J Biochem Cell Biol 42(1):5–12. https://doi.org/10.1016/j.biocel.2009.10.006

3. Bhutto I, Lutty G (2012) Understanding age-related macular degeneration (AMD): relationships between the photoreceptor/retinal pigment epithelium/Bruch's membrane/choriocapillaris complex. Mol Asp Med 33(4):295–317. https://doi.org/10.1016/j.mam.2012.04.005

4. Campochiaro PA (2015) Molecular pathogenesis of retinal and choroidal vascular diseases. Prog Retin Eye Res 49:67–81

5. Osaadon P, Fagan XJ, Lifshitz T, Levy J (2014) A review of anti-VEGF agents for proliferative diabetic retinopathy. Eye 28(5):510–520. https://doi.org/10.1038/eye.2014.13

6. Writing committee for the diabetic retinopathy clinical research network, Gross JG, Glassman AR, Jampol LM, Inusah S, Aiello LP, Antoszyk AN, Baker CW, Berger BB, Bressler NM, Browning D, Elman MJ, Ferris FL, Friedman SM 3rd, Marcus DM, Melia M, Stockdale CR, Sun JK, Beck RW (2015). Panretinal photocoagulation vs intravitreous ranibizumab for proliferative diabetic retinopathy: a randomized clinical trial. JAMA 314(20):2137–2146. https://doi.org/10.1001/jama.2015.15217

7. Lally DR, Gerstenblith AT, Regillo CD (2012) Preferred therapies for neovascular age-related macular degeneration. Curr Opin Ophthalmol 23(3):182–188. https://doi.org/10.1097/ICU.0b013e328352411c

8. Holz FG, Amoaku W, Donate J, Guymer RH, Kellner U, Schlingemann RO, Weichselberger A, Staurenghi G, Group SS (2011) Safety and efficacy of a flexible dosing regimen of ranibizumab in neovascular age-related macular degeneration: the SUSTAIN study. Ophthalmology 118(4):663–671. https://doi.org/10.1016/j.ophtha.2010.12.019

9. Rofagha S, Bhisitkul RB, Boyer DS, Sadda SR, Zhang K, S-US Group (2013) Seven-year outcomes in ranibizumab-treated patients in ANCHOR, MARINA, and HORIZON: a multicenter cohort study (SEVEN-UP). Ophthalmology 120(11):2292–2299. https://doi.org/10.1016/j.ophtha.2013.03.046

10. Falavarjani KG, Nguyen QD (2013) Adverse events and complications associated with intravitreal injection of anti-VEGF agents: a review of literature. Eye 27(7):787–794. https://doi.org/10.1038/eye.2013.107

11. Pike SE, Yao L, Jones KD, Cherney B, Appella E, Sakaguchi K, Nakhasi H, Teruya-Feldstein J, Wirth P, Gupta G, Tosato G (1998) Vasostatin, a calreticulin fragment, inhibits angiogenesis and suppresses tumor growth. J Exp Med 188(12):2349–2356

12. Yao L, Pike SE, Setsuda J, Parekh J, Gupta G, Raffeld M, Jaffe ES, Tosato G (2000) Effective targeting of tumor vasculature by the angiogenesis inhibitors vasostatin and interleukin-12. Blood 96(5):1900–1905

13. Sheu SJ, Bee YS, Ma YL, Liu GS, Lin HC, Yeh TL, Liou JC, Tai MH (2009) Inhibition of choroidal neovascularization by topical application of angiogenesis inhibitor vasostatin. Mol Vis 15:1897–1905

14. Bee YS, Sheu SJ, Ma YL, Lin HC, Weng WT, Kuo HM, Hsu HC, Tang CH, Liou JC, Tai MH (2010) Topical application of recombinant calreticulin peptide, vasostatin 48, alleviates laser-induced choroidal neovascularization in rats. Mol Vis 16:756–767

15. Bee YS, Tu L, Sheu SJ, Lin HC, Tang JH, Wang JH, Prea SM, Dusting GJ, Wu DC, Zhong J, Bui BV, Tai MH, Liu GS (2017) Gene delivery of calreticulin anti-angiogenic domain attenuates the development of choroidal neovascularization in rats. Hum Gene Ther. https://doi.org/10.1089/hum.2016.035

16. Petit L, Khanna H, Punzo C (2016) Advances in gene therapy for diseases of the eye. Hum Gene Ther 27(8):563–579

17. Rakoczy EP, Lai CM, Magno AL, Wikstrom ME, French MA, Pierce CM, Schwartz SD, Blumenkranz MS, Chalberg TW, Degli-Esposti MA, Constable IJ (2015) Gene therapy with recombinant adeno-associated vectors for neovascular age-related macular degeneration: 1 year follow-up of a phase 1 randomised clinical trial. Lancet 386(10011):2395–2403. https://doi.org/10.1016/S0140-6736(15)00345-1

18. Heier JS, Kherani S, Desai S, Dugel P, Kaushal S, Cheng SH, Delacono C, Purvis A, Richards S, Le-Halpere A, Connelly J, Wadsworth SC, Varona R, Buggage R, Scaria A, Campochiaro PA (2017) Intravitreous injection of AAV2-sFLT01 in patients with advanced neovascular age-related macular degeneration: a phase 1, open-label trial. Lancet 390(10089):50–61. https://doi.org/10.1016/s0140-6736(17)30979-0

19. Pike SE, Yao L, Setsuda J, Jones KD, Cherney B, Appella E, Sakaguchi K, Nakhasi H, Atreya CD, Teruya-Feldstein J, Wirth P, Gupta G, Tosato G (1999) Calreticulin and calreticulin fragments are endothelial cell inhibitors that suppress tumor growth. Blood 94(7):2461–2468

20. Xiao F, Wei Y, Yang L, Zhao X, Tian L, Ding Z, Yuan S, Lou Y, Liu F, Wen Y, Li J, Deng H, Kang B, Mao Y, Lei S, He Q, Su J, Lu Y, Niu T, Hou J, Huang MJ (2002) A gene therapy for cancer based on the angiogenesis inhibitor, vasostatin. Gene Ther 9(18):1207–1213. https://doi.org/10.1038/sj.gt.3301788

21. Lange-Asschenfeldt B, Velasco P, Streit M, Hawighorst T, Pike SE, Tosato G, Detmar M (2001) The angiogenesis inhibitor vasostatin does not impair wound healing at tumor-inhibiting doses. J Investig Dermatol 117(5):1036–1041. https://doi.org/10.1046/j.0022-202x.2001.01519.x

22. Huegel R, Velasco P, De la Luz Sierra M, Christophers E, Schroder JM, Schwarz T, Tosato G, Lange-Asschenfeldt B (2007) Novel anti-inflammatory properties of the angiogenesis inhibitor vasostatin. J Investig Dermatol 127(1):65–74. https://doi.org/10.1038/sj.jid.5700484

23. Tang J, Kern TS (2011) Inflammation in diabetic retinopathy. Prog Retin Eye Res 30(5):343–358

24. Datta S, Cano M, Ebrahimi K, Wang L, Handa JT (2017) The impact of oxidative stress and inflammation on RPE degeneration in non-neovascular AMD. Prog Retin Eye Res. https://doi.org/10.1016/j.preteyeres.2017.03.002

25. Liu GS, Wang JH, Lee JH, Tsai PJ, Tsai HE, Sheu SJ, Lin HC, Dusting GJ, Tai MH, Bee YS (2015) Gene delivery by subconjunctival injection of adenovirus in rats: a study of local distribution transgene duration and safety. PloS one 10(12):e0143956. https://doi.org/10.1371/journal.pone.0143956

26. McCarty DM (2008) Self-complementary AAV vectors; advances and applications. Mol Ther J Am Soc Gene Ther 16(10):1648–1656. https://doi.org/10.1038/mt.2008.171

27. Kong F, Li W, Li X, Zheng Q, Dai X, Zhou X, Boye SL, Hauswirth WW, Qu J, Pang JJ (2010) Self-complementary AAV5 vector facilitates quicker transgene expression in photoreceptor and retinal pigment epithelial cells of normal mouse. Exp Eye Res 90(5):546–554. https://doi.org/10.1016/j.exer.2010.01.011

28. Dalkara D, Kolstad KD, Caporale N, Visel M, Klimczak RR, Schaffer DV, Flannery JG (2009) Inner limiting membrane barriers to AAV-mediated retinal transduction from the vitreous.

Mol Ther J Am Soc Gene Ther 17(12):2096–2102. https://doi.org/10.1016/j.ymthe.2016.10.008

29. Takahashi K, Igarashi T, Miyake K, Kobayashi M, Yaguchi C, Iijima O, Yamazaki Y, Katakai Y, Miyake N, Kameya S, Shimada T, Takahashi H, Okada T (2017) Improved intravitreal AAV-mediated inner retinal gene transduction after surgical internal limiting membrane peeling in cynomolgus monkeys. Mol Ther J Am Soc Gene Ther 25(1):296–302

30. Maguire AM, Simonelli F, Pierce EA, Pugh EN Jr, Mingozzi F, Bennicelli J, Banfi S, Marshall KA, Testa F, Surace EM, Rossi S, Lyubarsky A, Arruda VR, Konkle B, Stone E, Sun J, Jacobs J, Dell'Osso L, Hertle R, Ma JX, Redmond TM, Zhu X, Hauck B, Zelenaia O, Shindler KS, Maguire MG, Wright JF, Volpe NJ, McDonnell JW, Auricchio A, High KA, Bennett J (2008) Safety and efficacy of gene transfer for Leber's congenital amaurosis. N Engl J Med 358(21):2240–2248

31. MacLaren RE, Groppe M, Barnard AR, Cottriall CL, Tolmachova T, Seymour L, Clark KR, During MJ, Cremers FP, Black GC, Lotery AJ, Downes SM, Webster AR, Seabra MC (2014) Retinal gene therapy in patients with choroideremia: initial findings from a phase 1/2 clinical trial. Lancet 383(9923):1129–1137

32. Lai CM, Estcourt MJ, Himbeck RP, Lee SY, Yew-San Yeo I, Luu C, Loh BK, Lee MW, Barathi A, Villano J, Ang CL, van der Most RG, Constable IJ, Dismuke D, Samulski RJ, Degli-Esposti MA, Rakoczy EP (2012) Preclinical safety evaluation of subretinal AAV2.sFlt-1 in non-human primates. Gene Ther 19(10):999–1009. https://doi.org/10.1038/gt.2011.169

33. Dalkara D, Byrne LC, Klimczak RR, Visel M, Yin L, Merigan WH, Flannery JG, Schaffer DV (2013) In vivo-directed evolution of a new adeno-associated virus for therapeutic outer retinal gene delivery from the vitreous. Sci Transl Med 5(189):189ra176. https://doi.org/10.1126/scitranslmed.3005708

34. Ip MS, Scott IU, Brown GC, Brown MM, Ho AC, Huang SS, Recchia FM (2008) Anti-vascular endothelial growth factor pharmacotherapy for age-related macular degeneration: a report by the American Academy of Ophthalmology. Ophthalmology 115(10):1837–1846. https://doi.org/10.1016/j.ophtha.2008.08.012

35. Nguyen QD, Brown DM, Marcus DM, Boyer DS, Patel S, Feiner L, Gibson A, Sy J, Rundle AC, Hopkins JJ, Rubio RG, Ehrlich JS (2012) Ranibizumab for diabetic macular edema: results from 2 phase III randomized trials: RISE and RIDE. Ophthalmology 119(4):789–801. https://doi.org/10.1016/j.ophtha.2011.12.039

36. Curtis LH, Hammill BG, Schulman KA, Cousins SW (2010) Risks of mortality, myocardial infarction, bleeding, and stroke associated with therapies for age-related macular degeneration. Arch Ophthalmol 128(10):1273–1279. https://doi.org/10.1001/archophthalmol.2010.223 **(Chicago, Ill: 1960)**

37. Avery RL, Gordon GM (2016) Systemic safety of prolonged monthly anti-vascular endothelial growth factor therapy for diabetic macular edema: a systematic review and meta-analysis. JAMA Ophthalmol 134(1):21–29. https://doi.org/10.1001/jamaophthalmol.2015.4070

38. McCarty DM, Monahan PE, Samulski RJ (2001) Self-complementary recombinant adeno-associated virus (scAAV) vectors promote efficient transduction independently of DNA synthesis. Gene Ther 8(16):1248–1254. https://doi.org/10.1038/sj.gt.3301514

39. Liu GS, Tsai HE, Weng WT, Liu LF, Weng CH, Chuang MR, Lam HC, Wu CS, Tee R, Wen ZH, Howng SL, Tai MH (2011) Systemic pro-opiomelanocortin expression induces melanogenic differentiation and inhibits tumor angiogenesis in established mouse melanoma. Hum Gene Ther 22(3):325–335. https://doi.org/10.1089/hum.2010.090

40. Carpentier G, Martinelli M, Courty J, Cascone I (2012) Angiogenesis analyzer for ImageJ. In: 4th ImageJ User and developer conference proceedings, Mondorf-les-Bains, Luxembourg

41. Deliyanti D, Miller AG, Tan G, Binger KJ, Samson AL, Wilkinson-Berka JL (2012) Neovascularization is attenuated with aldosterone synthase inhibition in rats with retinopathy. Hypertension 59(3):607–613. https://doi.org/10.1161/hypertensionaha.111.188136

42. Livak KJ, Schmittgen TD (2001) Analysis of relative gene expression data using real-time quantitative PCR and the 2(-Delta Delta C(T)) Method. Methods 25(4):402–408. https://doi.org/10.1006/meth.2001.1262

43. Connor KM, Krah NM, Dennison RJ, Aderman CM, Chen J, Guerin KI, Sapieha P, Stahl A, Willett KL, Smith LE (2009) Quantification of oxygen-induced retinopathy in the mouse: a model of vessel loss, vessel regrowth and pathological angiogenesis. Nat Protoc 4(11):1565–1573

44. Nivison-Smith L, Zhu Y, Whatham A, Bui BV, Fletcher EL, Acosta ML, Kalloniatis M (2014) Sildenafil alters retinal function in mouse carriers of retinitis pigmentosa. Exp Eye Res 128:43–56. https://doi.org/10.1016/j.exer.2014.08.014

Affiliations

Leilei Tu[1,2] · Jiang-Hui Wang[2,3] · Veluchamy A. Barathi[4,5,6] · Selwyn M. Prea[7] · Zheng He[7] · Jia Hui Lee[2] · James Bender[8] · Anna E. King[8] · Grant J. Logan[9] · Ian E. Alexander[9,10] · Youn-Shen Bee[11] · Ming-Hong Tai[12] · Gregory J. Dusting[2,3] · Bang V. Bui[7] · Jingxiang Zhong[1] · Guei-Sheung Liu[1,2,3,13,14]

1 Department of Ophthalmology, The First Affiliated Hospital of Jinan University, Guangzhou, Guangdong, China

2 Centre for Eye Research Australia, Royal Victorian Eye and Ear Hospital, East Melbourne, VIC, Australia

3 Ophthalmology, Department of Surgery, University of Melbourne, Melbourne, VIC, Australia

4 Translational Pre-clinical Model Platform, Singapore Eye Research Institute, Singapore National Eye Centre, Singapore, Singapore

5 Department of Ophthalmology, Yong Loo Lin School of Medicine, National University of Singapore, Singapore, Singapore

6 Ophthalmology and Visual Sciences Academic Clinical Program, DUKE-NUS Graduate Medical School, Singapore, Singapore

7 Department of Optometry and Vision Sciences, University of Melbourne, Parkville, VIC, Australia

8 Wicking Dementia Research and Education Centre, University of Tasmania, Hobart, TAS, Australia

9 Gene Therapy Research Unit, Children's Medical Research Institute and Sydney Children's Hospitals Network, University of Sydney, Sydney, NSW, Australia

10 Discipline of Child and Adolescent Health, University of Sydney, Westmead, NSW, Australia

[11] Department of Ophthalmology, Kaohsiung Veterans General Hospital, Kaohsiung, Taiwan

[12] Institute of Biomedical Sciences, National Sun Yat-Sen University, Kaohsiung, Taiwan

[13] Menzies Institute for Medical Research, University of Tasmania, Hobart, TAS, Australia

[14] Liverpool St, Hobart, TAS 7000, Australia